International Journal of Environmental Science and Technology (2023) 20:11049–11060
https://doi.org/10.1007/s13762-023-05099-x

ORIGINAL PAPER

Experimental study of oxytetracycline degradation using Fenton-like processes

S. Yildiz[1] · H. Mihçiokur[2] · A. Olabi[1]

Received: 26 September 2022 / Revised: 2 May 2023 / Accepted: 11 July 2023 / Published online: 31 July 2023

Abstract

This study aimed to investigate the degradation efficiency of Oxytetracycline (OTC) using different Fenton processes. Fe^{2+} and nZVI reagents were used as Fenton reagents. To compare the effect on OTC degradation, Fenton process (FP), photo-Fenton process (P-FP), sono-Fenton process (S-FP) and sono–photo-Fenton process (S–P-FP) were applied. In addition, degradation products formed after OTC degradation by these methods, in which Fe^{2+} and nZVI reagents were used separately, were detected. UV-A, UV-B and UV-C lamps were used as UV light source. S-FP and S–P-FP used ultrasound with a frequency of 40 kHz and a power of 180 watts. In the use of Fe^{2+} and nZVI, the OTC removal efficiency (η) was determined as 45.64% and 50.28% for FP respectively, and in P-FP was 62.75%, 66.42% for UV-A light, 67.69%, 66.96% for UV-B, and 60.40%, 69.67% for UV-C. The η values were found as 86.30%, 87.75% (for UV-A), 90.28%, 89.55% (for UV-B) and 84.48%, 93.05% (for UV-C) in S–P-FP with ultrasound added. For S-FP, the η value recorded 74.86% and 77.51% for Fe^{2+} and nZVI application, respectively. The degradation products detected in the OTC different oxidation method were generally the same. The degradation product to be considered here is 2-Isopropyl-5-methyl-1-heptanol. LC50 and EC50 values of this product were quite low compared to other degradation products and OTC.

Keywords Oxytetracycline · UV · Fenton · Degradation products

Introduction

As a result of the production and use of antibiotics, a large amount of antibiotic-containing wastewater is generated. These waters are discharged into the environment, causing significant pollution (Focazio et al. 2008). Tetracycline antibiotics have been of interest to researchers as they are broad-spectrum antibiotics against both gram-positive and gram-negative bacteria and are widely used (Ge et al. 2018). Oxytetracycline (OTC), a broad-spectrum antibiotic from the tetracycline group, is widely used for the prevention and treatment of diseases in livestock (Shen et al. 2019).

OTCs cannot be treated with conventional wastewater treatment methods such as physical adsorption, chemical reactions, and biodegradation due to their tenacity and chemical stability (Cha and Carlson 2019, Li et al. 2015). Therefore, more effective treatment methods need to be developed to remove OTC from water (Liu et al. 2016).

In researches on the treatment of OTC wastewater, methods such as photochemical degradation (Liu et al. 2015), advanced oxidation processes (AOPs) (Fan et al. 2022; Varank et al. 2022; Yan et al. 2021; Espindola et al. 2019; Liu et al. 2016; Pereira, et al. 2014), electrocatalytic oxidation (Ghodsi et al. 2016), membrane separation (Garcia-Rodriguez et al., 2015), bioelectrochemistry (Yan et al. 2018), natural aluminosilicate and carbon nanotubes (Morales-Serrato et al. 2022), ozone process (Li et al. 2008) and gamma radiation (Lopez Penalver et al. 2013) have been used.

AOPs is an environmentally friendly technology for removing stubborn pollutants (Ramírez-Pereda et al. 2018). Among AOPs, interest in the Fenton process (FP) is increasing due to its simplicity of operation (Tang and Wang 2018). FP is used to generate ·OH radicals from Fe^{2+} in the

Editorial responsibility: Samareh Mirkia.

✉ S. Yildiz
sayiteryildiz@gmail.com

[1] Department of Environmental Engineering, Engineering Faculty, Sivas Cumhuriyet University, 58140 Sivas, Turkey

[2] Department of Environmental Engineering, Engineering Faculty, Erciyes University, 38280 Kayseri, Turkey

presence of H_2O_2 according to Eqs. 1–3 (Wang and Zhuan 2020; Luo et al. 2010).

$$Fe^{2+} + H_2O_2 \rightarrow Fe^{3+} + \cdot OH + OH^- \quad (1)$$

$$\cdot OH + H_2O_2 \rightarrow \cdot HO_2 + H_2O \quad (2)$$

$$2 \cdot OH \rightarrow H_2O_2 \quad (3)$$

Recently, nanoscale zero-valent iron (nZVI) has been widely used, especially for the treatment of organic pollutants, due to its properties such as high specific surface area and large reducing reaction capacity (Fu et al. 2013). Through the reaction between dissolved oxygen and Fe^0, H_2O_2 is produced (Eq. 4) and thus Fe^{2+} is formed. In addition, nZVI particles form hydrogen molecules through the reaction in Eq. (5) (Tran et al. 2020).

$$Fe^0 + O_2 + 2H^+ \rightarrow H_2O_2 + Fe^{2+} \quad (4)$$

$$Fe^0 + 2H_2O \rightarrow Fe^{2+} + H_2 + 2OH^- \quad (5)$$

Fenton process with UV light is called the photo-Fenton process (P-FP). UV light used in the process has a positive effect on the direct formation of ·OH radicals (Feng et al. 2003). It has also been stated that ultrasonic irradiation can accelerate the degradation reaction in the Fenton process (Chen et al. 2011). In this context, ultrasound-integrated Fenton processes such as sono-Fenton (S-FP) and sono-photo-Fenton (S–P-FP) are alternatives for OTC degradation studies.

The Purpose of this study:

(i) To determine low concentrations of Fenton reagents suitable for degradation of OTC.
(ii) To compare the effect of Fe^{2+} and nZVI used as Fenton reagent on OTC degradation.
(iii) To determine the effects of FP, P-FP, S-FP and S–P-FP on the degradation of OTC.
(iv) To identify by-products resulting from OTC degradation by Fenton and Fenton-like processes.

This study is very important especially in terms of providing the opportunity to compare the use of nZVI and Fe^{2+} in different Fenton processes. Furthermore, the study is unique in that it examines OTC degradation using different processes, reveals the effect of these processes separately, and determines the by-products that arise at the end of the processes. All experiments were performed three times due to experimental error (standard deviation ≤ 5%).

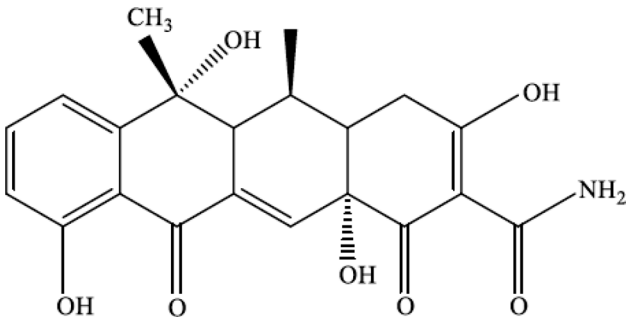

Fig. 1 Chemical structure of OTC

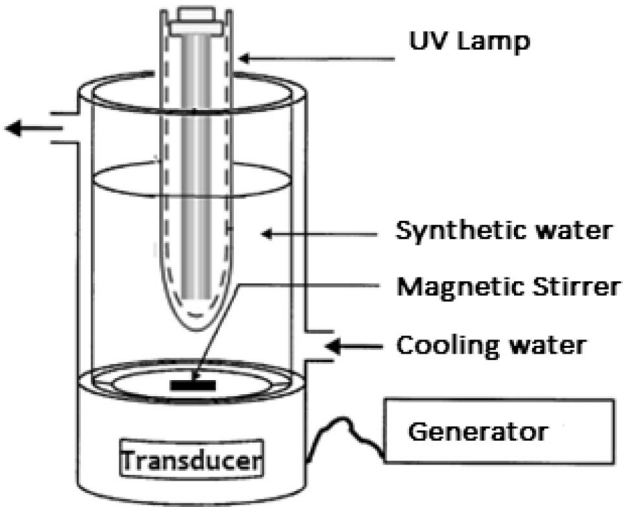

Fig. 2 Schematic view of reactor

Materials and methods

Experimental study

Oxytetracycline hydrochloride ($C_{22}H_{24}N_2O_9$.HCl, purity > 99%) were purchased from Sigma-Aldrich. Chemical structure of OTC is shown in Fig. 1 (Wu et al. 2018). Iron (II) chloride tetrahydrate ($FeCl_2.4H_2O$, purity: 98%) and hydrogen peroxide (H_2O_2, 35% v/v) were used as Fenton reagents. UV-A (365 nm), UV-B (302 nm), UV-C (256 nm) lamps were used as UV light source. Ultrasound studies were carried out by applying ultrasound with a frequency of 40 kHz and a power of 180 watts. pH measurements were made with Adwa AD8000 brand device. The study was carried out in a custom-built reactor. Figure 2 depicts a schematic of the reactor.

In order to determine the wavelengths at which drug active ingredients make maximum absorbance,

Hach-Lange DR 5000 brand spectrophotometer was used for each drug active ingredient in the range of 200–400 nm, for 10 mg/L active ingredient concentration, 1 cm beam path length and spectral band width of 1 nm. Wavelength scan was performed. As a result of the wavelength scans, it was determined at which wavelength the measurements of the drug active substances would be made.

The removal efficiency (η) of OTC was calculated using the OTC concentration before and after the reaction according to Eq. 6:

$$\eta(\%) = \frac{C_0 - C_e}{C_0} x100 \quad (6)$$

where η (%) represents the OTC removal efficiency, C_0 (mg/L) represents the initial OTC concentration, and C_e (mg/L) represents the OTC concentration after reaction.

Stock solutions were prepared daily from the active ingredients and the desired concentrations were obtained by making the necessary dilutions. Oxytetracycline active ingredient gave two characteristic peaks at 354 nm and 266 nm. It was seen that the wavelengths at which oxytetracycline active substance makes maximum absorbance in wavelength scans are in accordance with the values in the literature (Gallego and Arroyo 2002; Prasad and Rao 2010). Then, calibration curves were created for each of the wavelengths at which it had maximum absorbance and measurements were carried out.

Preparation of nZVI (Fe^0)

5.34 g of $FeCl_2.4H_2O$ was mixed in 30 mL of solution (24 mL of ethanol + 6 mL of distilled water). In addition, 1 M $NaBH_4$ was prepared by dissolving 3.05 g of $NaBH_4$ in 100 mL of distilled water. The $NaBH_4$ solution was added dropwise to the Fe solution and mixed in a mixer for 10 min. After the resulting black mud was separated by centrifugation, it was washed with 25 mL of ethanol, centrifuged again and dried at 50 °C (Olabi and Yildiz 2021). The obtained material was kept in a desiccator and used in the experiments.

The specific surface area of nZVI particles is substantially greater than that of conventional iron (Mueller et al. 2012). The nitrogen adsorption–desorption isotherms of nZVI are shown in Fig. 3 and changes in the Particle Size of nZVI are seen in Table 1 (Yildiz and Olabi 2021). The

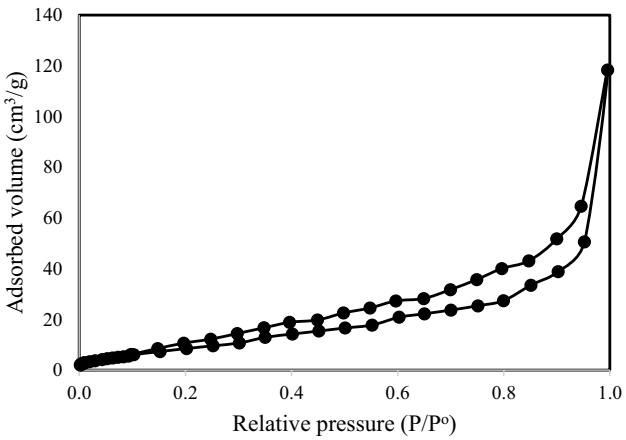

Fig. 3 The nitrogen adsorption–desorption isotherm of Fe^0

Table 1 The surface area and pore characteristics of Fe^0

	Fe^0
S_{BET}[a] (m^2/g)	37.69
V_{Total}[b] (cm^3/g)	0.184
V_{micro}[c] (cm^3/g)	0.012
D_p[d] (Å)	97.36

[a]Multipoint BET method; [b]Volume adsorbed at $P/P^o = 0.99$; [c]Micropore volume calculated by DR method; [d]Average pore diameter determined by DFT

adsorption–desorption isotherms of sample are of type III (BET classification) according to the IUPAC classification, indicating that the samples comprise micro- and mesoporous particles. As shown in Table 1, the acid-activated nZVI was found to have high surface area and mesopore volumes (Yildiz and Olabi 2021).

Degradation products detection

After oxytetracycline was degraded by Fenton and Fenton like processes, degradation products were observed in the GC/MS device (Shimadzu GCMS-QP 2010) (Zhao et al. 2021). Rxi 5 SIL MS capillary column with 30 m length, 0.25 mm diameter and 1 µm film thickness was used in the device. Helium gas of 99.999% purity was used as the carrier gas at a flow rate of 2.10 mL/min. The injection port was operated at splitless mode. The oven temperature was

brought from 40 to 240 °C in 20 min by heating at a rate of 10 °C/min and was kept at 240 °C for 10 min.

Toxicity evaluation of degradation products

In this study, toxicity calculations were made using the ECOSAR module of the EPI SuiteTM software developed by EPA (US, Environmental Protection Agency) and SRC (Syracuse Research Corp.) (US EPA 2012). The EPI Suite software is based on Quantitative Structure–Activity Relationships (QSARs) methodologies used to estimate toxicity measurements from the physical properties of chemicals based on their molecular structures and to estimate the effects of chemicals on biota (US EPA 2012). In order to have information about the toxicity of degradation products and Oxytetracycline, the lowest LC50 (50% Lethal Concentration) and EC50 (50% effective concentration) values were determined.

Results and discussion

Effect of Fe^{2+} and nZVI

To achieve perfect OTC degradation, it is necessary to determine the optimal conditions that balance the initial OTC concentration, H_2O_2 content, and catalyst dosage (Pham et al. 2018). To reveal the effect of nZVI and Fe^{2+} on the Fenton treatment, the iron concentration was varied between 1, 2, 4, 6, 8, 10, 12 mg/L (Fig. 4). Removal efficiency of OTC increased with the increase of iron content. No increase was observed for Fe^{2+} and nZVI after 8 mg/L. When the catalyst dosage increased from 1 to 10 mg/L, the η value increased from 8.1 to 27.76% in Fe^{2+} and from 12.55 to 31% in nZVI. The reason for this is the formation of a large amount of active sites, which causes an increase in ·OH through the decomposition of H_2O_2 and promotes the degradation of organic pollutants (Whang and Zhuan 2020). The main reactions took place according to Eqs. 1–3.

Higher amount of Fe^{3+} ions (Eq. 7) formed as a result of higher Fe^{2+} and nZVI concentration can react with H_2O_2 (Eq. 8) and consequently reduce the degradation efficiency (Zouanti et al. 2020). In the study, when the concentration increased to 12 mg/L, η value decreased slightly and became 25.20% and 25.34% for Fe^{2+} and nZVI, respectively. Similar observations at higher Fe^{2+} concentration have been reported in other studies (Elmolla and Chaudhuri 2009; Mansour et al. 2012).

$$Fe^{2+} + \cdot OH \rightarrow Fe^{3+} + OH^- \quad (7)$$

$$Fe^{3+} + H_2O_2 \rightarrow Fe^{2+} + \cdot HO_2 + H^+ \quad (8)$$

Effect of H_2O_2

Hydrogen peroxide is the key component in the catalytic reaction to produce ·OH (Xu and Wang 2012). The effect of

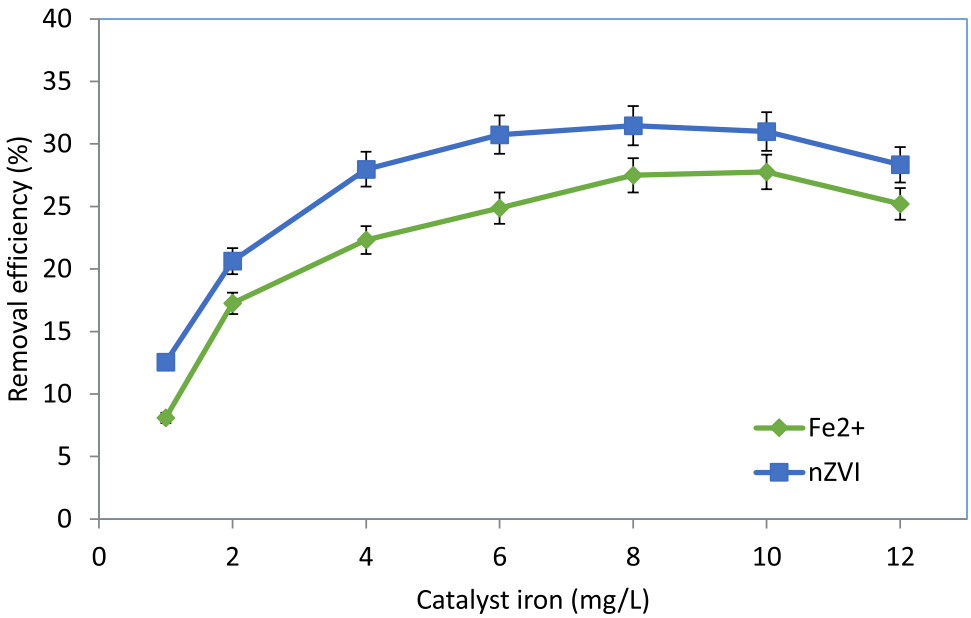

Fig. 4 Effect of catalyst iron on degradation. Conditions: OTC concentration 10 mg/L, pH 4, H_2O_2 60 mg/L, time 60 min

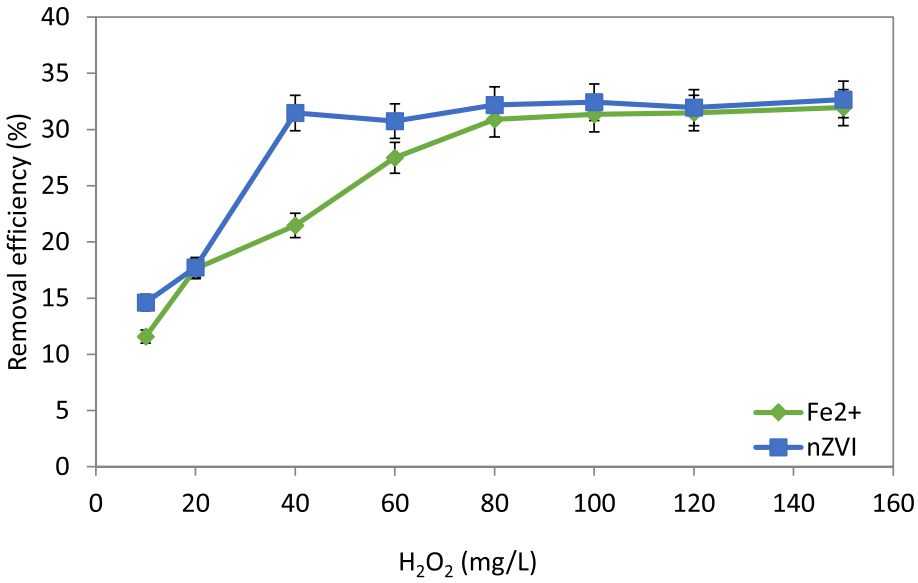

Fig. 5 Effect of H_2O_2 on degradation. Conditions: OTC concentration 10 mg/L, pH 4, Fe^{2+} 8 mg/L, nZVI 6 mg/L, time 60 min

different H_2O_2 concentrations (10, 20, 40, 60, 80, 100, 120, 150 mg/L) on OTC degradation is given in Fig. 5. With the increase in H_2O_2, the η value also increased. However, despite the increasing amount, there was no significant change in the degradation efficiency after 80 mg/L H_2O_2. For Fe^{2+} and nZVI, η values at 10 mg/L H_2O_2 were 11.59%, 14.60%, for 40 mg/L H_2O_2 21.47%, 31.46%, and at 80 mg/L H_2O_2 30.89%, 32.19%, respectively. At 150 mg/L H_2O_2, the η value was determined as 31.95% and 32.67%, respectively.

The rate at which ·OH radicals decompose OTC molecules is much slower than the rate of decomposition of H_2O_2 into ·OH radicals. In addition, ·OH radicals are scavenged and consumed during reactions with other ·OH radicals (Yu et al. 2014). When the H_2O_2 concentration is above the critical value, the ·OH produced can be captured by excess H_2O_2 to form the less active O_2H radical (Eqs. 9–11) (Buxton et al. 1988), resulting in a loss of activity in OTC removal (Li et al. 2020).

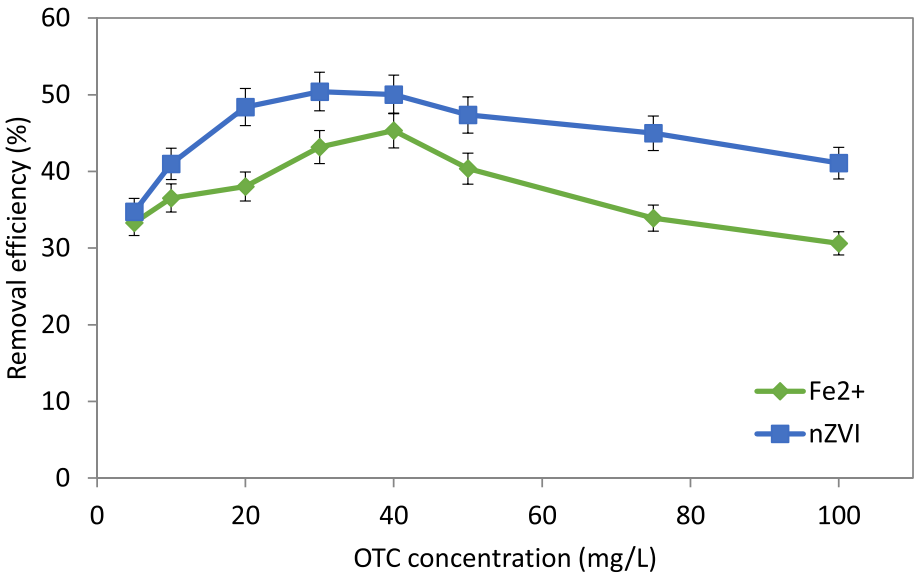

Fig. 6 Effect of OTC concentration on degradation. Conditions: pH 4; Fe^{2+} 8 mg/L, H_2O_2 80 mg/L; nZVI 6 mg/L, H_2O_2 40 mg/L; time 60 min

$$H_2O_2 + \cdot OH \rightarrow H_2O + \cdot O_2H \quad (9)$$

$$O_2H + \cdot OH \rightarrow H_2O + O_2 \quad (10)$$

$$OH + OH \rightarrow H_2O_2 \quad (11)$$

Effect of the initial OTC concentration

The effect of OTC concentration (5, 10, 20, 30, 40, 50, 75, 100 mg/L) on degradation efficiency was investigated, keeping the operating conditions unchanged (Fig. 6). As the initial concentration increased from 5 to 40 mg/L, the η value increased from 33.30 to 45.34% for Fe^{2+} and from 34.75 to 50% for nZVI. However, the η value decreased with increasing concentration. The η value for Fe^{2+} and nZVI at 50 mg/L concentration was 40.37% and 47.35% respectively, while it dropped to 30.62% and 41.07% at 100 mg/L concentration.

As the concentration of OTC increases, the potential for contact and exposure to fixed amounts of ·OH decreases. This situation causes more ·OH consumption and consequently a decrease in removal efficiency (Zazouli and Taghavi 2012). Also, higher OTC concentrations result in the formation of more intermediates that compete with OTC to react with ·OH and can also become limiting reagents (Zouanti et al. 2020).

Effect of the initial pH

In the study, the effect on OTC degradation by changing the pH between 2 and 8 was investigated and the results are given in Fig. 7. The positively charged form (OTC^+) dominates under acidic conditions, the molecular form (OTC^0) under neutral conditions, and the negatively charged form (OTC^- and OTC^{2-}) under alkaline conditions. The stability of OTC^+ is much stronger than OTC^0, OTC^- and OTC^{2-} (Zhang et al. 2018). In this study, there was a significant decrease in the η value when the pH value increased above 4. The η values for Fe^{2+} and nZVI at pH 2 were 22.07%, 31.90 respectively, while they recorded 30.89% and 31.47% at pH 3. The highest degradation efficiency was obtained at pH 4, as the η values for Fe^{2+} and nZVI were determined as 36.53% and 41%, respectively. The η values recorded 18.46%, 24.82% at pH 6 and 3.76% and 2.80% at pH 8 for Fe^{2+} and nZVI respectively.

The pH values of 3 and below negatively affect the reaction of H_2O_2 with Fe^{2+}, causing a decrease in ·OH production. The low η value at pH 2 may be due to ·OH scavenging of H^+ ions. (Eq. 12). On the other hand, at pH > 4, OTC degradation efficiency decreases due to precipitation of dissolved iron (Eqs. 13 and 14) in the presence of high concentrations of OH^- ions (Lucas and Peres 2006).

$$\cdot OH + H^+ + e^- \rightarrow H_2O \quad (12)$$

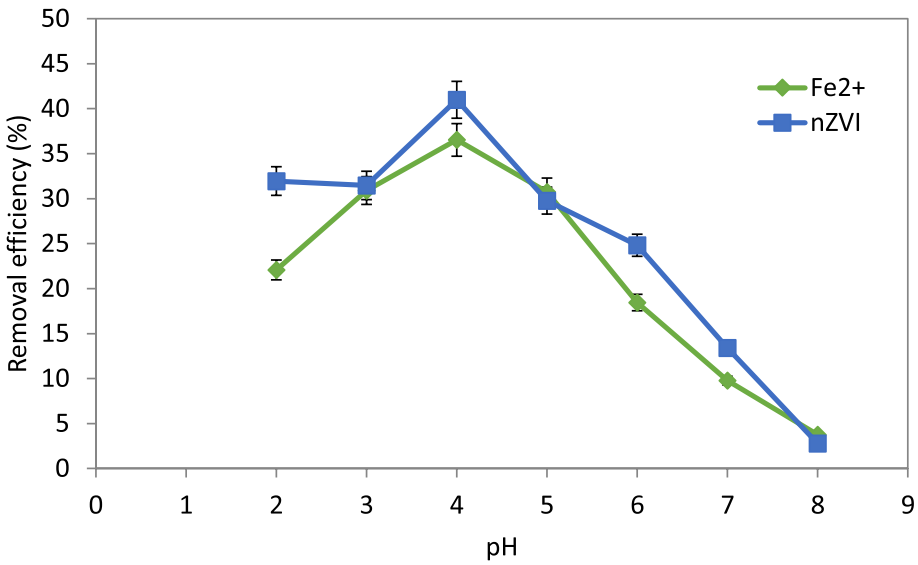

Fig. 7 Effect of pH on degradation. Conditions: concentration OTC 10 mg/L; Fe^{2+} 8 mg/L, H_2O_2 80 mg/L; nZVI 6 mg/L, H_2O_2 40 mg/L; time 60 min

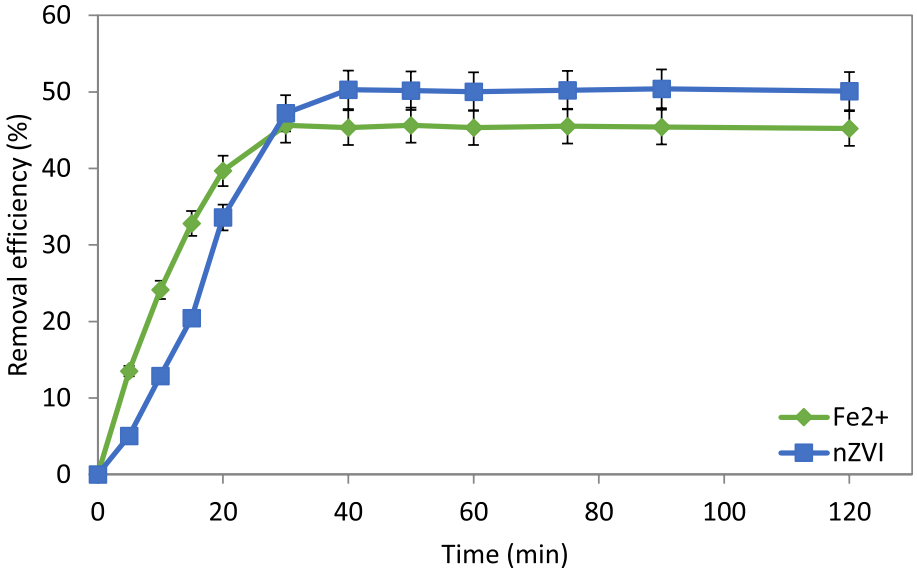

Fig. 8 Effect of reaction time on degradation. Conditions: concentration OTC 10 mg/L; pH 4; Fe^{2+} 8 mg/L, H_2O_2 80 mg/L; nZVI 6 mg/L, H_2O_2 40 mg/L; pH 4

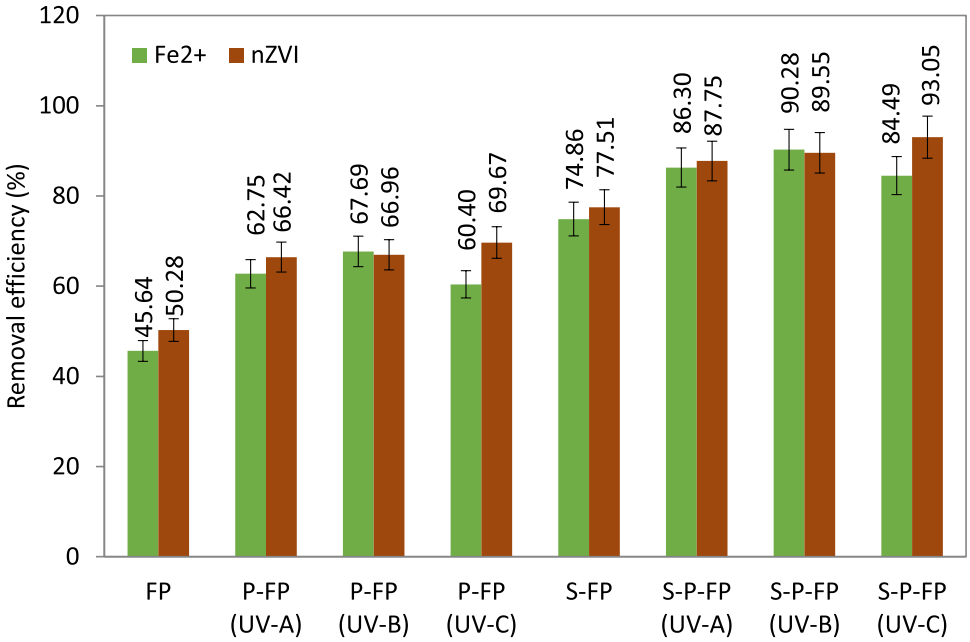

Fig. 9 Effect of different fenton process on degradation. Conditions: concentration OTC 10 mg/L; pH 4; Fe^{2+} 8 mg/L, H_2O_2 80 mg/L; nZVI 6 mg/L, H_2O_2 40 mg/L; time 60 min

$$Fe^{2+} + 2OH^- \rightarrow Fe(OH)_2 \quad (13)$$

$$Fe^{3+} + 3OH^- \rightarrow Fe(OH)_3 \quad (14)$$

Effect of the reaction time

To determine the optimum reaction time, treatment was performed at 5, 10, 15, 20, 30, 40, 50, 60, 75, 90, 120 min (Fig. 8). Since ·OH is rapidly produced by the reaction of Fe^{2+} and H_2O_2, the Fenton reaction usually occurs very quickly at the beginning of the process (Mirzaei et al. 2017). The η values for Fe^{2+} and nZVI were calculated as 13.53% and 5.04% after 5 min, 45.64% and 47.20 after 30 min, 45.34% and 50.04 after 60 min, and 45.22% and 50.10% after 120 min, respectively.

As seen in Fig. 8, the OTC degradation process consisted of two stages. The first is the Fe^{2+}/H_2O_2 stage, and the ·OH formed at this stage degrades OTC very quickly. The second stage is the Fe^{3+}/H_2O_2 stage in which the oxidation rate is

slower than the first stage due to the slow regeneration of Fe^{2+} from Fe^{3+}. Therefore, complete mineralization cannot be achieved at this stage (Alverez-Gallegos and Pletcher 1999).

Photo Fenton/sono-Fenton/sono–photo Fenton processes

In order to determine the effect of different Fenton processes on OTC degradation, P-FP (Fe^{2+}/nZVI + H_2O_2 + UV-A/B/C), S-FP (Fe^{2+}/nZVI + H_2O_2 + US) and S–P-FP (Fe^{2+}/nZVI + H_2O_2 + UV-A/B/C + US) were carried out in a batch reactor. OTC removal efficiencies of all processes are given in Fig. 9.

In the photolysis process (P-FP), the degradation of organic compounds occurs by reactive species such as ·OH, $\cdot HO_2$, ·O and $\cdot O_2^-$, which are formed according to Eqs. 15–17 in the presence of UV, providing the required photon energy (hv) (Elles et al. 2007).

$$H_2O + hv \rightarrow H_2O \quad (15)$$

$$H_2O \rightarrow \cdot OH + \cdot H \quad (16)$$

$$H_2O^+ + H_2O \rightarrow \cdot OH + H_3O^+ \quad (17)$$

In this study, η values for Fe^{2+} and nZVI in P-FP treatment were 62.75%, 66.42% with UV-A light, 67.69%, 66.96% with UV-B light, and 60.40% and 69.67% with UV-C light, respectively.

Ultrasound waves cause micro-sized bubbles to form, grow, and eventually collapse in aqueous solution (Chauhan et al. 2021). The ultrasound creates a cycle of compression and dilution, alternatively increasing the pressure

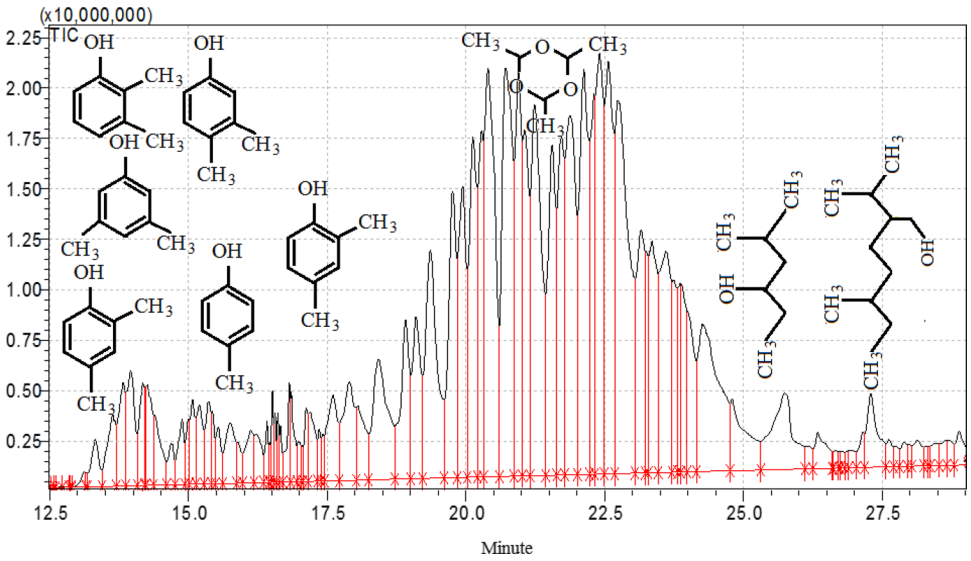

Fig. 10 Chromatogram obtained as a result of Fenton process with $Fe.^{2+}$. 13–18 min (1,3-dimethyl- Phenol, 3,4-dimethyl-, Phenol, 3,5-dimethyl, Phenol, 2,3-dimethyl, Phenol, 2,4-dimethyl, Phenol, p-Cresol), 20–22,5 min (s-Trioxane, 2,4,6-triethyl-), 24,5–25,5 min (2,4 Dimethyl-3-hexanol), 26,5–27,5 min (2-Isopropyl-5-methyl-1-heptanol)

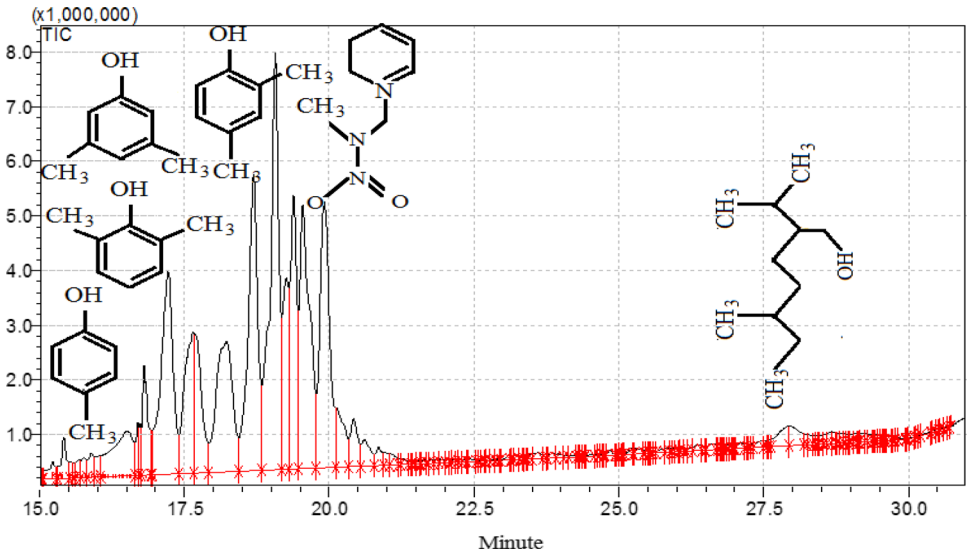

Fig. 11 Chromatogram obtained as a result of Fenton process with nZVI. 15–16 min (p-Cresol), 16,5–19 min (Phenol, 3,5-dimethyl-, Phenol, 2,4-dimethyl-, Phenol, 2,6-dimethyl-) 19, 5-21 min (Methanamine, N-nitro-N-(1-piperidylmethyl)-), 26,5–27,5 min (2-Isopropyl-5-methyl-1-heptanol)

Table 2 The lowest LC50 and EC50 values of degradation products and OTC

OTC and degredation product	Fenton process	Lowest EC50 and LC50 (mg/L) with organism	
		EC50	LC50
Oxytetracycline	–	7.952/Green algae	4.442/Daphnid
1,3-dimethyl- Phenol	Fe^{2+}	4.506/Lemna gibba	2.892/Daphnid
3,4-dimethyl-, Phenol	Fe^{2+}	4.506/Lemna gibba	2.892/Daphnid
3,5-dimethyl, Phenol	Fe^{2+}/ nZVI	4.506/Lemna gibba	2.892/Daphnid
2,3-dimethyl, Phenol	Fe^{2+}	4.506/Lemna gibba	2.892/Daphnid
2,4-dimethyl, Phenol	Fe^{2+}/ nZVI	4.506/Lemna gibba	2.892/Daphnid
p-Cresol	Fe^{2+}/ nZVI	11.910/Lemna gibba	5.229/ Daphnid
s-Trioxane2,4,6-triethyl-	Fe^{2+}	46.216/Green algae	58.158/Daphnid
2,4 Dimethyl-3-hexanol	Fe^{2+}	17.814/Green algae	19.128/Daphnid
2-Isopropyl-5-methyl-1-heptanol	Fe^{2+}/ nZVI	2.252/Green algae	0.471/Mysid
2,6-dimethyl, Phenol	nZVI	4.506/Lemna gibba	2.892/Daphnid
Methanamine, N-nitro-N-(1-piperidyl-methyl)-)	nZVI	35.692/Green algae	29.569/Daphnid

in the aqueous solution. This results in rupture of the cavitation bubble and produce of short-lived free radicals (·OH, ·H and $\cdot HO_2$) (Verma et al. 2014). As seen in Fig. 9, the η value in the S-FP treatment was 74.86% and 77.51 for Fe^{2+} and nZVI, respectively. The degradation efficiency can be increased by hybridizing the sonolysis process with other AOPs (Chauhan et al. 2021). Several literatures have indicated that the combination of US and UV shows a positive effect (Na et al. 2012; Duran et al. 2013). In this study, the degradation efficiency also increased significantly in S–P-FP. The η values for Fe^{2+} and nZVI were 86.30% and 87.75% with UV-A light, 90.28% and 89.55% with UV-B light and 84.49% and 93.05% with UV-C light, respectively.

Degradation products

In this study, it was tried to determine the degradation products formed after OTC was degraded by different Fenton processes. The degradation products detected in eight different Fenton processes are generally the same. Since the degradation products are similar, two sample chromatograms obtained for the Fenton processes (with Fe^{2+} and with nZVI) processes, as in Figs. 10 and 11, instead of all chromatograms.

With the help of the obtained chromagrams and the GC/MS device library, degradation products were detected. Then, the LC50 and EC50 values of the degradation products were determined and compared with OTC. The lowest LC50 and EC50 values of degradation products and OTC are as in Table 2.

The EC 50 and LC 50 values of Dimethyl and phenol forms were approximately half of that of OTC. This shows that the toxicity of these products is higher than that of OTC. However, it should be noted that degradation products will always be less than the OTC concentration in quantity. Degradation products occur as a result of the fragmentation of OTC. In addition, LC50 and EC50 values of 2-Isopropyl-5-methyl-1-heptanol are quite low compared to other degradation products and OTC. This product is the most toxic intermediate. For this reason, its concentration should be monitored continuously after degradation processes.

Many reaction pathways have been proposed for the theoretical degradation of OTC. In addition, different intermediates were obtained in different experimental studies (Saha et al. 2020; Shang et al. 2015; Wei et al. 2022; Mohan et al. 2020; Liu et al. 2016; Hwang et al. 2013). Therefore, comparisons regarding toxicity should relate to the main component and intermediates. Intermediates obtained in other studies may differ. Intermediate products depend on the type of degradation process, its performance, temperature, pH and many other variables.

Conclusion

In this study, OTC degradation was performed in FP, P-FP, S-FP and S–P-FP processes using Fe^{2+} and nZVI under different experimental conditions. Variables such as pH, OTC concentration, H_2O_2, Fe^{2+} and nZVI doses and reaction time were used to determine optimum conditions. Fenton oxidation was performed under conditions of: OTC concentration

10 mg/L, pH 4; Fe^{2+} 8 mg/L, H_2O_2 80 mg/L; nZVI 6 mg/L, H_2O_2 40 mg/L. In the application of Fe^{2+} and nZVI, the η values were 45.64% and 50.28% for FP, respectively, and in P-FP were 62.75%, 66.42% for UV-A light, 67.69%, 66.96% for UV-B, and 60.40%, 69.67 for UV-C. The η values in S–P-FP were 86.30%, 87.75% (for UV-A), 90.28%, 89.55% (for UV-B) and 84.48%, 93.05% (for UV-C). In S-FP, the η value was 74.86% and 77.51% with the use of Fe^{2+} and nZVI, respectively.

In the study, no difference was observed in degradation products formed after degrading with different Fenton methods using OTC, Fe^{2+} and nZVI. Furthermore, there was no significant difference between OTC and degradation products in terms of EC50 and LC50 values at the mg/L level. The degradation product to be considered here is 2-Isopropyl-5-methyl-1-heptanol. LC50 and EC50 values of this product were quite low compared to other degradation products and OTC. Fenton and Fenton-like processes could be very promising and reliable technology for OTC degradation. Comparison of different iron reagents (Fe^{2+}, nZVI) and determination of degradation products resulting from OTC degradation distinguish this study from other studies and make it important.

In this study, while experimenting for the effect of one factor, the other factors were kept constant, which is the normal procedure in conventional experiment designs. However, simultaneous optimization of all factors is possible using statistically designed experiments, with designs generated on computers using software. Comparing the results of 'one factor at a time' experiments such as the one undertaken in this study, with that of simultaneous optimization experiments will be important for the method selection of future studies.

Acknowledgment The authors wish to thank all who assisted in conducting this work.

Author contributions SY and HM designed the study. Material preparation and analysis were performed by AO and HM. The first draft of the manuscript was written by SY, while all authors commented on it. All authors read and approved the final manuscript.

Declarations

Conflict of interest The authors declare that they have no known competing financial interests or personal relationships that could have appeared to influence the work reported in this paper.

References

Alverez-Gallegos A, Pletcher D (1999) The removal of low level organics via hydrogen peroxide formed in a reticulated vitreous carbon cathode cell. Part 2: The removal of phenols and related compounds from aqueous effluents. Electrochimica Acta 44(14):2483–2492

Buxton GV, Greenstock CL, Helman WP, Ross AB (1988) Critical review of rate constants for reactions of hydrated electrons, hydrogen atoms and hydroxyl radicals (·OH/·O in aqueous solution. J Phys Chem Ref Data 17(2):513–886

Cha J, Carlson KH (2019) Biodegradation of veterinary antibiotics in lagoon waters. Process Saf Environ Prot 127:306–313

Chauhan R, Dinesh GK, Alawa B, Chakma S (2021) A critical analysis of sono-hybrid advanced oxidation process of ferrioxalate system for degradation of recalcitrant pollutants. Chemosphere 277:130324

Chen B, Wang X, Wang C, Jiang W, Li S (2011) Degradation of azo dye direct sky blue 5B by sonication combined with zero-valent iron. Ultrason Sonochem 18(5):1091–1096

Duran A, Monteagudo JM, Sanmartín I, Carrasco A (2013) Solar photo-Fenton mineralization of antipyrine in aqueous solution. J Environ Manag 130:64–71

Elles CG, Shkrob IA, Crowell RA, Bradforth SE (2007) Excited state dynamics of liquid water: insight from the dissociation reaction following two-photon excitation. J Chem Phys 126(16):164503

Elmolla E, Chaudhuri M (2009) Optimization of Fenton process for treatment of amoxicillin, ampicillin and cloxacillin antibiotics in aqueous solution. J Hazard Mater 170(2–3):666–672

Espindola JC, Cristovao RO, Santos SGS, Boaventura RAR, Dias MM, Lopes JCB, Vilar VJP (2019) Intensification of heterogeneous TiO_2 photocatalysis using the NETmix mili-photoreactor under microscale illumination for oxytetracycline oxidation. Sci Total Environ 681:467–474

Fan QQ, Niu CG, Guo H, Huang DW, Dong ZT, Yang YY, Qin MZ (2022) Insights into the role of reactive oxygen species in photocatalytic H_2O_2 generation and OTC removal over a novel BN/$Zn_3In_2S_6$ heterojunction. J Hazard Mater 438:129483

Feng J, Hu X, Yue PL, Zhu HY, Lu GQ (2003) Discoloration and mineralization of reactive red HE-3B by heterogeneous photo-Fenton reaction. Water Res 37(15):3776–3784

Focazio MJ, Kolpin DW, Barnes KK, Furlong ET, Meyer MT, Zaugg SD, Barber LB, Thurman ME (2008) A national reconnaissance for pharmaceuticals and other organic wastewater contaminants in the United States—II. Untreated drinking water sources. Sci Total Environ 402:201–216

Fu F, Ma J, Xie L, Tang B, Han W, Lin S (2013) Chromium removal using resin supported nanoscale zero-valent iron. J Environ Manag 128:822–827

Gallego JML, Arroyo JP (2002) Spectrophotometric determination of hydrocortisone, nystatin and oxytetracycline in synthetic and pharmaceutical preparations based on various univariateand multivariate methods. Anal Chim Acta 460:85–97

Garcia-Rodríguez A, Matamoros V, Kolev SD, Fontàs C (2015) Development of a polymer inclusion membrane (PIM) for the preconcentration of antibiotics in environmental water samples. J Membr Sci 492:32–39

Ge L, Dong Q, Halsall C, Chen CEL, Li J, Wang D, Zhang P, Yao Z (2018) Aqueous multivariate phototransformation kinetics of dissociated tetracycline: implications for the photochemical fate in surface waters. Environ Sci Pollut Res 25:15726–15732

Ghodsi J, Rafati AA, Shoja Y (2016) First report on electrocatalytic oxidation of oxytetracycline by horse radish peroxidase: application in developing a biosensor to oxytetracycline determination. Sens Actuators B Chem 224:692–699

Hwang SA, Lee KB, Cho JY (2013) Degradation of veterinary antibiotic oxytetracycline using electron ionizing energy. J Korean Soc Appl Biol Chem 56(6):759–762

Li K, Yediler A, Yang M, Schulte-Hostede S, Wong MH (2008) Ozonation of oxytetracycline and toxicological assessment of its oxidation by-products. Chemosphere 72(3):473–478

Li R, Jia Y, Wu J, Zhen Q (2015) Photocatalytic degradation and pathway of oxytetracycline in aqueous solution by Fe_2O_3–TiO_2 nanopowder. RSC Adv 5(51):40764–40771

Li X, Cui K, Guo Z, Yang T, Cao Y, Xian Y, Xi M (2020) Heterogeneous Fenton-like degradation of tetracyclines using porous magnetic chitosan microspheres as an efficient catalyst compared with two preparation methods. Chem Eng J 379:122324

Liu Y, He X, Duan X, Fu Y, Dionysiou DD (2015) Photochemical degradation of oxytetracycline: influence of pH and role of carbonate radical. Chem Eng J 276:113–121

Liu Y, He X, Fu Y, Dionysiou DD (2016) Degradation kinetics and mechanism of oxytetracycline by hydroxyl radical-based advanced oxidation processes. Chem Eng J 284:1317–1327

Lopez Penalver JJ, Gomez Pacheco CV, Sanchez Polo M, Rivera Utrilla J (2013) Degradation of tetracyclines in different water matrices by advanced oxidation/reduction processes based on gamma radiation. J Chem Technol Biotechnol 88(6):1096–1108

Lucas MS, Peres JA (2006) Decolorization of the azo dye reactive black 5 by Fenton and photo-Fenton oxidation. Dyes Pigment 71(3):236–244

Luo W, Zhu L, Wang N, Tang H, Cao M, She Y (2010) Efficient removal of organic pollutants with magnetic nanoscaled $BiFeO_3$ as a reusable heterogeneous Fenton-like catalyst. Environ Sci Technol 44:1786–1791

Mansour D, Fourcade F, Bellakhal N, Dachraoui M, Hauchard D, Amrane A (2012) Biodegradability improvement of sulfamethazine solutions by means of an electro-Fenton process. Water Air Soil Pollut 223(5):2023–2034

Mirzaei A, Chen Z, Haghighat F, Yerishalmi L (2017) Removal of pharmaceuticals from water by homo/heterogonous Fenton-type processes—a review. Chemosphere 174:665–688

Mohan H, Lim JM, Lee SW, Cho M, Park YJ, Seralathan KK, Oh BT (2020) V_2O_5/RGO/Pt nanocomposite on oxytetracycline degradation and pharmaceutical effluent detoxification. J Chem Technol Biotechnol 95(1):297–307

Morales-Serrato DA, Torres-Pérez J, de Jesús R-B, Reyes-López SY (2022) Effect of Zn nanoparticles doping on oxytetracycline removal by natural aluminosilicate and carbon nanotubes. Water Air Soil Pollut 233(2):1–21

Mueller NC, Braun J, Bruns J, Černík M, Rissing P, Rickerby D, Nowack B (2012) Application of nanoscale zero valent iron (NZVI) for groundwater remediation in Europe. Environ Sci Pollut Res 19(2):550–558

Na S, Jinhua C, Cui M, Khim J (2012) Sonophotolytic diethyl phthalate (DEP) degradation with UVC or VUV irradiation. Ultrason Sonochem 19(5):1094–1098

Olabi A, Yildiz S (2021) Sludge disintegration using UV assisted sono-Fenton process. Environ Sci Pollut Res 28(37):52565–52575

Pereira JHOS, Queiros DB, Reis AC, Nunes OC, Borges MT, Boaventura RAR, Vilar VJP (2014) Process enhancement at near neutral pH of a homogeneous photo-Fenton reaction using ferricarboxylate complexes: application to oxytetracycline degradation. Chem Eng J 253:217–228

Pham VL, Kim DG, Ko SO (2018) Oxidative degradation of the antibiotic oxytetracycline by Cu@ Fe_3O_4 core-shell nanoparticles. Sci Total Environ 631:608–618

Prasad ARG, Rao VS (2010) Spectrophotometric methods for the microdetermination of oxytetracycline and hostacycline. Sci World J 5(1):1–4

Ramírez-Pereda B, Alvarez-Gallegos A, Rangel-Peraza JG, Bustos-Terrones YA (2018) Kinetics of acid orange 7 oxidation by using carbon fiber and reticulated vitreous carbon in an electro-Fenton process. J Environ Manag 213:279–287

Saha N, McGaughy K, Held MA, Reza MT (2020) Hydrothermal degradation of β-estradiol and oxytetracycline at selective reaction severities. SN Appl Sci 2(9):1–9

Shang Z, Salim AA, Khalil Z, Quezada M, Bernhardt PV, Capon RJ (2015) Viridicatumtoxins: expanding on a rare tetracycline antibiotic scaffold. J Org Chem 80(24):12501–12508

Shen Y, Chu L, Zhuan R, Xiang X, Sun H, Wang J (2019) Degradation of antibiotics and antibiotic resistance genes in fermentation residues by ionizing radiation: a new insight into a sustainable management of antibiotic fermentative residuals. J Environ Manag 232:171–178

Tang J, Wang J (2018) Metal organic framework with coordinatively unsaturated sites as efficient Fenton-like catalyst for enhanced degradation of sulfamethazine. Environ Sci Technol 52(9):5367–5377

Tran ML, Nguyen CH, Van Tran TT, Juang RS (2020) One-pot synthesis of bimetallic Pt/nZVI nanocomposites for enhanced removal of oxytetracycline: roles of morphology changes and Pt catalysis. J Taiwan Inst Chem Eng 111:130–140

US Environmental Protection Agency (EPA) (2012) Estimation program interface suite™ for Microsoft® windows, version 4.11. United States environmental protection agency, Washington, DC, USA

Varank G, Can-Güven E, Guvenc SY, Garazade N, Turk OK, Demir A, Cakmakci M (2022) Oxidative removal of oxytetracycline by UV-C/hydrogen peroxide and UV-C/peroxymonosulfate: process optimization, kinetics, influence of co-existing ions, and quenching experiments. J Water Process Eng 50:103327

Verma A, Sangwan P, Dixit D (2014) Sonophotocatalytic degradation studies of alizarin reactive red dye. Arab J Sci Eng 39(11):7477–7482

Wang J, Zhuan R (2020) Degradation of antibiotics by advanced oxidation processes: an overview. Sci Total Environ 701:135023

Wei ZS, Chen XL, Huang ZS, Jiao HY, Xiao XL (2022) Insights into the removal of gaseous oxytetracycline by combined ozone and membrane biofilm reactor. Environ Eng Res 27(6):210469

Wu Y, Yue Q, Gao Y, Ren Z, Gao B (2018) Performance of bimetallic nanoscale zero-valent iron particles for removal of oxytetracycline. J Environ Sci 69:173–182

Xu L, Wang J (2012) Magnetic nanoscaled Fe_3O_4/CeO_2 composite as an efficient Fenton-like heterogeneous catalyst for degradation of 4-chlorophenol. Environ Sci Tech 46(18):10145–10153

Yan W, Guo Y, Xiao Y, Wang S, Ding R, Jiang J, Gang H, Wang H, Yang J, Zhao F (2018) The changes of bacterial communities and antibiotic resistance genes in microbial fuel cells during long-term oxytetracycline processing. Water Res 142:105–114

Yan T, Ping Q, Zhang A, Wang L, Dou Y, Li Y (2021) Enhanced removal of oxytetracycline by UV-driven advanced oxidation with peracetic acid: Insight into the degradation intermediates and N-nitrosodimethylamine formation potential. Chemosphere 274:129726

Yildiz S, Olabi A (2021) Effect of Fe^{2+} and Fe^0 applied photo-Fenton processes on sludge disintegration. Chem Eng Technol 44(1):95–103

Yu C, Li G, Wei L, Fan Q, Shu Q, Yu JC (2014) Fabrication, characterization of β-MnO_2 microrod catalysts and their performance

in rapid degradation of dyes of high concentration. Catal Today 224:154–162

Zazouli MA, Taghavi M (2012) Phenol removal from aqueous solutions by electrocoagulation technology using iron electrodes: effect of some variables. J Water Resour Prot 4:980–983

Zhang YH, Shi J, Xu ZW, Chen Y, Song DM (2018) Degradation of tetracycline in a schorl/H_2O_2 system: proposed mechanism and intermediates. Chemosphere 202:661–668

Zhao W, Dong Q, Sun C, Xia D, Huang H, Yang G, Leung DY (2021) A novel Au/g-C3N4 nanosheets/CeO2 hollow nanospheres plasmonic heterojunction photocatalysts for the photocatalytic reduction of hexavalent chromium and oxidation of oxytetracycline hydrochloride. Chem Eng J 409:128185

Zouanti M, Bezzina M, Dhib R (2020) Experimental study of degradation and biodegradability of oxytetracycline antibiotic in aqueous solution using Fenton process. Environ Eng Res 25(3):316–323